Anal. Bioanal. Electrochem., Vol. 14, No. 7, 2022, 715-729

Analytical & Bioanalytical Electrochemistry

2022 by CEE
www.abechem.com

Full Paper

The Selectivity and Stability of Epithelial Sodium Channel (ENaC) Aptamer as an Electrochemical Aptasensor

Egista I. Fazrin[1], Arum Kurnia Sari[1], Riyanto Setiyono[1], Shabarni Gaffar[1], Yulia Sofiatin[2], Husein H. Bahti[1], and Yeni Wahyuni Hartati[1]*

[1]*Department of Chemistry, Faculty of Mathematics and Natural Sciences, Universitas Padjadjaran, Indonesia*
[2]*Department of Public Health, Faculty of Medicine, Universitas Padjadjaran, Indonesia*

*Corresponding Author, Tel.: +628122132349
E-Mail: yeni.w.hartati@unpad.ac.id

Received: 14 April 2022 / Received in revised form: 18 July 2022 / Accepted: 19 July 2022 / Published online: 31 July 2022

Abstract- Epithelial sodium channel (ENaC) proteins are proportional to sodium intake and clinically associated with hypertension. The selectivity of aptamer-based electrochemical biosensor for ENaC detection has been developed in this study, and the stability of the cerium oxide modified electrode was reported. The concentration of ENaC was measured using differential pulse voltammetry of $[Fe(CN)_6]^{4-/3-}$ redox system. The aptasensor based on the bioconjugate of ENaC aptamer with gold nanoparticle (AuNP) using streptavidin-biotin linker, and immobilized on the screen-printed electrode-CeO_2. The ENaC aptamer selectivity was tested for other proteins that might be present in the urine sample, and the stability of the modified SPCE was studied throughout storage of SPCE-CeO_2-aptamer. The limit of detection of ENaC protein with this aptasensor was obtained of 0.110 ng mL^{-1}, in the linear range of concentrations 0.05–3.0 ng mL^{-1}. The percentage of selectivity of the aptamer to ENaC compared to creatinine and potassium channel proteins was 79.08%. The cerium oxide modified SPCE/aptamer bioconjugate is stable up to one year of storage. The developed aptasensor is simple and can be miniaturized to determine the ENaC concentration in urine for the realization of a point-of-care device for the early detection of hypertension.

Keywords- Aptamer selectivity; Aptasensor stability; Epithelial Sodium Channel (ENaC); Electrochemical aptasensor; Hypertension biomarker; CeO_2 nanoparticles

1. INTRODUCTION

Hypertension is one of the most common non-communicable diseases and is a global public health problem, as serious complications, such as cardiovascular and renal disease, can arise from uncontrolled hypertension [1]. Blood pressure numbers of less than 120/80 mmHg are considered within the normal range [2]. According to the World Health Organization, hypertension complications account for 9.4 million deaths worldwide annually [3]. Hypertension is an abnormal increase in blood pressure, with a sustained increase causing damage to other organs such as the heart, kidneys, brain, etc. Many genes have been associated with blooa d pressure control or essential hypertension including epithelial sodium channel (ENaC), which are candidate genes in the salt-sensitive phenotype [4,5]. However, in most cases, the studies demonstrating positive associations correspond to an equal or larger number of studies showing a lack of association with a specific polymorphism [6]. Hypertension associated with high sodium levels can be detected by determining the amount of ENaC protein, as the higher the sodium concentration, the higher the ENaC protein activity to absorb sodium [7,8].

ENaC has been demonstrated to be involved in reabsorthe ption of filtered Na^+ in the distal nephron, including the aldosterone-sensitive distal nephron (ADSN) and the collecting duct [9]. ENaC protein is used as a biomarker of hypertension because it functions as the primary channel to control the level of renal sodium reabsorption, which is crucial for the regulation/homeostasis of the extracellular fluid volume, electrolyte balance, and long-term blood pressure [10]. There are several methods to detect ENaC protein, such as ELISA [4], electrochemical immunosensor [7,8], optical biosensor [11], and electrochemical aptasensor [12].

The use of an aptamer as a sensing element has numerous advantages because of its specific characteristics, such as high stability against increasing temperature, pH, and organic solvents, can recognize a variety of targets, high affinity, and specificity, efficiently interacting with large molecules such as proteins and cells, as well as small molecules such as nucleotides, organic dyes, amino acids, and metal ions [13-16]. An aptamer has been reported to have binding energy with ENaC protein of -206,94 $kJ.mol^{-1}$ as a result of in silico rational design [17].

To improve the sensitivity of an electrochemical aptasensor, there have been widely reported the use of nanomaterials as electrode modifiers, as well as biolements, such as the formation of bioconjugates. One of them is gold nanoparticles (AuNPs) which have acquired an imperative and noteworthy position in the field of clinical diagnostic methodologies and therapeutics [18]. The use of bioconjugates in electrochemical biosensors has been widely developed to accelerate the detection process and increase sensitivity. In addition, the use of bioconjugate with nanoparticles could enable the biosensors to be more selective and sensitive and increase the ratios of signal versus blank [7,19-21]. Gold nanoparticles can be directly

conjugated with bioelement through physical absorption and ionic or covalent bonding [22-26]. The formation of bioconjugates by adsorption of streptavidin on the AuNP surface has shown good results [27-29].

Modifying the electrodes is also one way to increase the sensitivity of an electrochemical biosensor. One modification of the carbon-based electrode with cerium oxide has been reported to result in better electrode performance due to the unique properties of cerium oxide such as good conductivity, and facilitating redox transfer properties [12,30,31]. CeO_2 is a choice that leads to astonishing catalytic reactivity owing to the extraordinary mobility of surface oxygen vacancies. Due to $Ce^{4+/}Ce^{3+}$ rearrangement, the oxygen vacancies modify the electronic and valence arrangement and potentially provide for the oxidation of carbonaceous species [32,33,34].

The use of a screen-printed carbon electrode (SPCE) electrochemically modified with CeO_2 has been successfully carried out by obtaining a low detection limit using the aptamer we designed [12,17]. However, the selectivity of the aptamer for several components that may be present in the urine sample such as creatinine and potassium channel protein, and the stability of the aptamer with respect to storage time have only been reported in this paper. The electrochemical aptasensor has been developed for the detection of ENaC protein using SPCE-CeO_2. The aptamer was formed into a bioconjugate with AuNP through the interaction of streptavidin-biotin, then the AuNP-aptamer bioconjugate was immobilized onto the surface of the SPCE-CeO_2 electrode via direct assembly. The optimum experimental conditions including aptamer concentration, incubation time of the AuNP-aptamer bioconjugate, and ENaC protein incubation time were determined.

2. EXPERIMENTAL SECTION

2.1. Chemicals and Apparatus

ENaC protein was obtained from Abcam, UK. Biotinylated- ENaC aptamer (sequence: 50–/5Biosg/CGG TGA GGT CGG GTC CAG TAG GCC TAC TGT TGA GTA GTG GGC TCC–30) was obtained from DT Integrated DNA Technologies, US. Streptavidin, potassium ferricyanide ($K_3[Fe(CN)_6]$), bovine serum albumin (BSA), cerium nitrate hexahydrate ($Ce(NO_3)_3.6H_2O$), and sodium citrate ($Na_3C_6H_5O_7$) were purchased from Sigma Aldrich. Potassium chloride (KCl) and phosphate buffer saline (PBS) pH 7.4 were obtained from Merck. The double-distilled water was produced by PT Ikapharmindo Putramas, Indonesia.

The electrochemistry measurements were conducted using a Zimmer & Peacock potentiostat connected to a computer using PST$_{RACE}$ 5.8 software (Zeamer & Peacock, UK). The SPCE (GSI Technologies, USA) was used as a working, auxiliary, and Ag/AgCl as a reference electrode for the electrochemical transducer. A scanning electron microscope (SEM) (JSM-6360-LA) was used for electrode surface morphology analysis. An FTIR (Pekin Elmer

Spectrum100) and UV-Vis spectrophotometer (Thermo Scientific, US) and Particle Size Analyzer (PSA) (HORIBA SZ-100) were used for the characterization of compounds. Other equipment used included centrifuges (Thermo Scientific MicroCL 17R, US), autoclave sterilizer (Prestige Medical SERIES 2100), hot plate (IKA C)-MAG HS7), magnetic stirrer, mini spin, micropipette (Eppendorf).

2.2. Preparation of gold nanoparticles colloids (AuNP)

The gold nanoparticles (AuNP) colloids were prepared by adding 10 mL of 0.5 mM chloroauric acid and stirring using a magnetic stirrer for 5 min, followed by the addition of 2 mL of 1% sodium citrate and continued stirring until the red wine-colored AuNP colloids formed [35]. The AuNP colloids were characterized by a visible spectrophotometer and PSA.

2.3. Preparation and characterization of the AuNP-aptamer bioconjugate

Firstly, 40 µL solution of streptavidin 50 µg mL^{-1} was added to 500 µL of 0.5 mM AuNPs colloid, then incubated in an ice bath for 1 hour. The solution was centrifuged for 30 minutes at 12,500 rpm, the supernatant was decanted and redissolved in 90 µL of double-distilled water. The AuNP-STV solution was regenerated with 20 µL of 0.5 µg.mL^{-1} biotinylated-aptamer solution, incubated for 30 minutes, centrifuged, and the supernatant removed. The AuNP-STV-biotinylated aptamer bioconjugate formed was characterized by a visible spectrophotometer, FTIR, and differential pulse voltammetry [26].

2.4. Characterization of the modified SPCE

The SPCE surface before (SPCE) and after modification (SPCE/CeO_2) was observed and the morphological features were characterized by SEM (JSM-6360-LA). FTIR measurements were performed on a Perkin Elmer Spectrum instrument set in the range limit of 450–4000 cm^{-1}. The CeO_2-modified SPCE was also electrochemically characterized by differential pulse voltammetry using a redox system of 10 mM $[Fe(CN)_6]^{4-/3-}$ containing 0.1 M KCl (in the potential range from −1.0 V to +1.0 V with a scanning rate of 0.008 V/s).

2.5. Optimization of parameters using the Box-Behnken method

The aptamer concentration ($\times_1$), bioconjugate incubation time ($\times_2$), and ENaC protein incubation time ($\times_3$) volume were optimized as shown in Table 1 (the lowest level −1, intermediate 0, and highest +1) using the Box-Behnken experimental design with Minitab 18.

Table 1. Factors influencing the experimental conditions using Box-Behnken of ENaC aptasensor

Factors	Unit	Level		
		-1	0	+1
aptamer concentration	μg mL^{-1}	0.5	1.0	1.5
bioconjugate incubation time	Minutes	10	20	30
ENaC protein incubation time	Minutes	5	10	15

2.6. Fabrication of the aptasensor

Briefly, 40 μL of 100 μg mL^{-1} of cerium nitrate was dropped onto the SPCE surface, followed by electrodeposition using differential pulse voltammetry from −1.0 V to +1.0 V and a scan rate of 0.05 V/s. The SPCE surface was rinsed with demineralized water and dried at room temperature. Then, 20 μL of bioconjugate was dropped onto the surface of the modified SPCE/CeO_2 electrode and incubated at room temperature for 30 min before being rinsed with PBS (pH 7.4) and dried at room temperature. The SPCE/CeO_2/bioconjugate was incubated in a 1% BSA solution at room temperature for 15 min, followed by rinsing with PBS (pH 7.4). Subsequently, 20 μL of ENaC solution was dropped onto the SPCE and incubated for 30 min at room temperature. The resulting aptasensor was electrochemically characterized by differential pulse voltammetry using a redox system of 10 mM ferricyanide containing 0.1 M KCl in the potential range from −1.0 to +1.0 V with a scanning rate of 0.008 V/s. The overall of bioelement modification and electron transfer process of ENaC aptasensor was shown in Scheme 1.

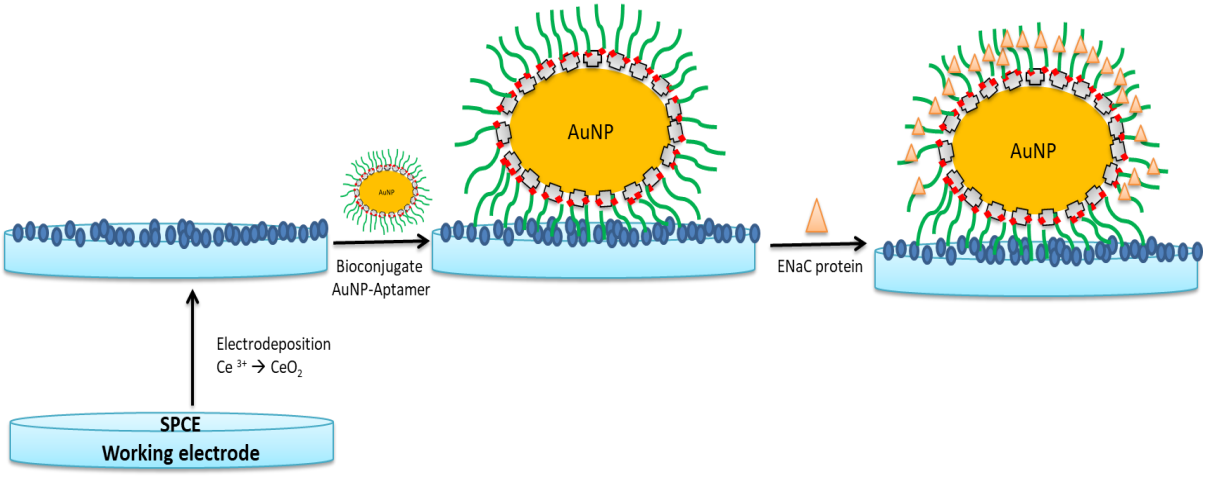

Scheme 1. Schematic illustration of the bioelement modification and electron transfer process of ENaC aptasensor

2.7. Calibration curves, detection limits, and quantification limits

Various concentrations of ENaC solutions (0.047; 0.094; 0.187; 0.375; 0.75; 1.5; and 3.0 ng mL^{-1}) were detected by the electrochemical aptasensor (differential pulse voltammetry using a redox system of 10 mM $[Fe(CN)_6]^{4-/3-}$ in 0.1 M KCl in the potential range of −1.0 V to +1.0 V with a scan rate of 0.008 V/s) using the optimal conditions determined from the Box-Behnken method. A linear curve of the concentration vs. the difference in average peak current (ΔI) for each measurement was used to determine the limit of detection and limit of quantification.

2.8. The study of ENaC aptamer selectivity

20 μL of creatinine, potassium channel, and ENaC proteins with a concentration of 1.5 g/mL were dripped on the CeO_2 modified SPCE/aptamer bioconjugate. Furthermore, the DPV measurement using the $[Fe(CN)_6]^{4-/3-}$ redox system. Signal change = $(I_0-I_1)/I_0$, where I_0 refers to the current before reduction and I_1 to the reduction current after incubation of the electrode with the target or interfering protein [36].

2.9. The study of stability of modified electrode

The SPCE-CeO_2/aptamer bioconjugates were stored for 1, 15, 30, 60, and 90 days at room temperature, and 1 month at 50°C. After being stored, 20 μL of 1% BSA was added, then it was rinsed using buffer, then the ENaC protein variation of concentration was added, and measured by DPV using the $[Fe(CN)_6]^{4-/3-}$ redox system. Then we analyzed the linearity and RSD value from each different storage time.

3. RESULTS AND DISCUSSION

3.1. Characterization of AuNPs and AuNP-Aptamer

Figure 1a showed the normalized spectra UV-Visible absorption of AuNPs. The color intensity of the AuNPs came from a photophysical response, which measured AuNP colloid had an absorption peak at a maximum wavelength of 521 nm. The colloidal AuNPs were synthesized by the chemical reduction of $HAuCl_4$ using sodium citrate with the reddish-purple color of the final reaction mixture indicates the formation of AuNPs. Sodium citrate acts as a reducing agent and stabilizer. Ion citrate has carboxylate (COO^-) and hydroxyl (OH) functional groups. The hydroxyl group will interact with the reduced gold so that the gold particles will be covered with negatively charged citrate ions. There will be a repulsive force between the gold particles, which can prevent the aggregation of AuNP. Adding citrate to the gold surface gives them some charge and helps stabilize them in water. It is also beneficial as it has a relatively low affinity for the gold surface and can be easily exchanged for something else. The surface charge of the surface adsorbed citric acid AuNPs would be negative, though the precise

number would depend on the conditions. The PSA data of the average nanoparticle size distribution was obtained of 33.8 nm as can be seen in Figures 1b and 1c.

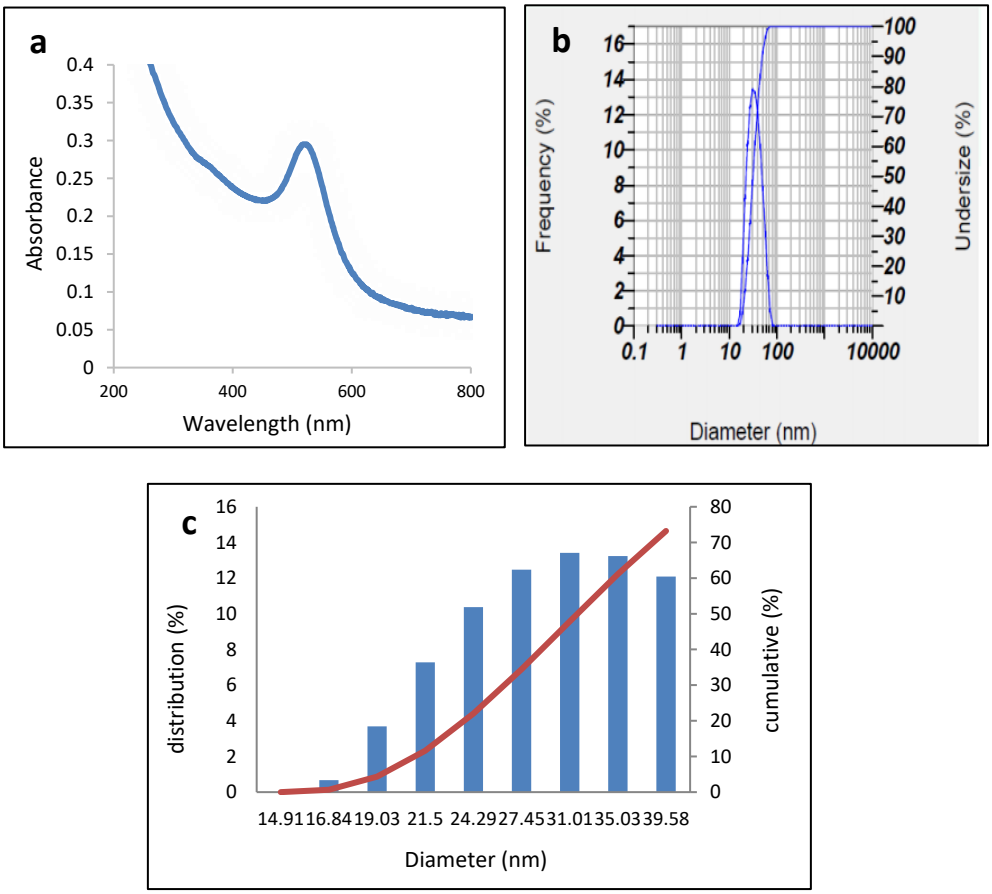

Figure 1. a) Characterization of AuNPs using a UV-VIS spectrophotometer with a maximum absorption wavelength of 521 nm, b) the DLS Spectra of AuNPs, c) the particle size distribution of AuNPs

The characterization of AuNP–Aptamer bioconjugates was shown in Figure 2. The UV-Visible absorption peaks were found at a wavelength of 529 nm for AuNPs and an additional peak at 260 nm for AuNP–Aptamer bioconjugates (Figure 2a). The changing shift in the AuNP peak from 521 nm to 529 nm in a peak intensity reflects the difference in colloid dispersion after AuNP functionalization as shown in Figure 2b. No significant peak expansion after functionalization, indicating that the addition of biomolecules to AuNP does not cause aggregation of the gold nanoparticles and make the AuNPs more stable. Figure 2c depicts the normalized Infra-red spectra of AuNPs and AuNP–Aptamer bioconjugates. Spectrum A related to streptavidin, there is an OH strain band at 3428.7 cm^{-1} and C=O strain at 1644.9 cm^{-1}, while spectrum B is related to the bioconjugate of AuNP-streptavidin, there is an OH strain band at 3418.8 cm^{-1} and C=O strain at 1644.6 cm^{-1}. These spectra indicate that the interaction of AuNP with the protein does not change the protein structure but causes a shift to a lower wavenumber

and a decrease in intensity. The formation of bioconjugate via physical adsorption between AuNP and streptavidin occurred due to AuNP, which has been stabilized by citrate ion, tends to be negatively charged, will do electrostatic interactions with the positively charged amino acid residues of streptavidin. The conjugation of a biotinylated-aptamer to AuNP-STV can increase the aptamer affinity and specificity in interacting with the target ENaC protein.

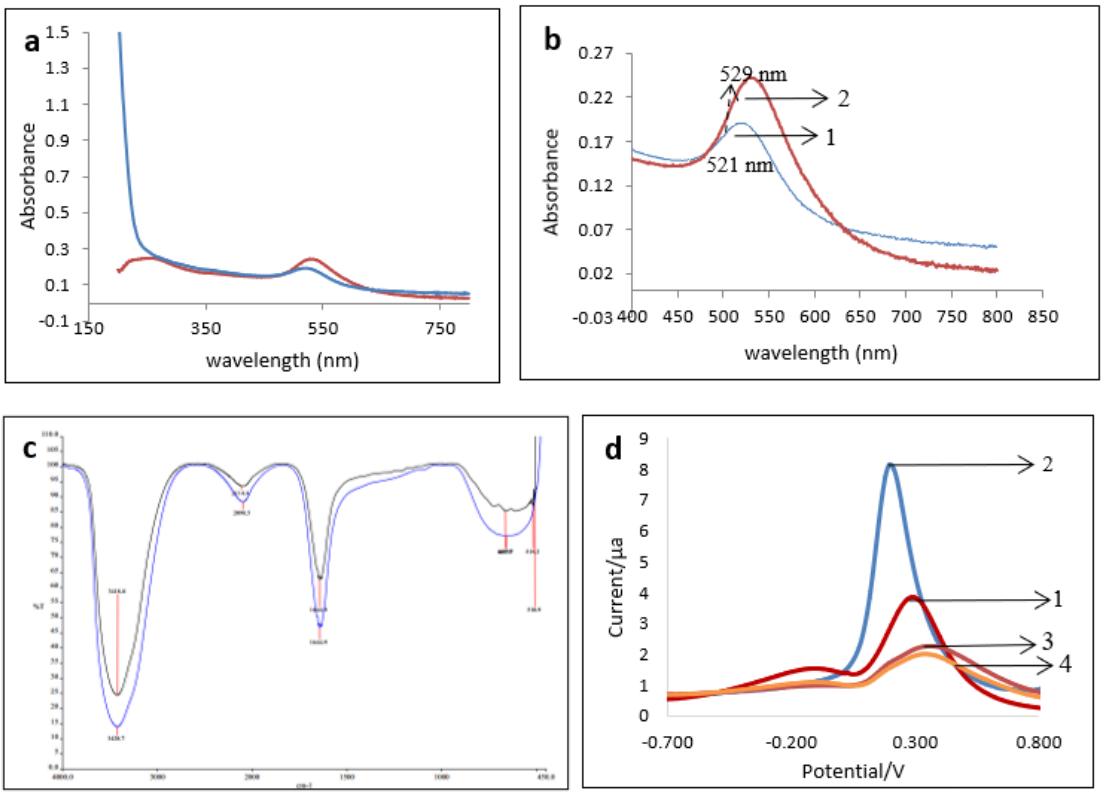

Figure 2. a) The UV-VIS spectra for AuNP and the bioconjugate, b) the spectra of (1) AuNP with λmax = 521 nm and (2) bioconjugate AuNP-aptamer with λ max = 529 nm, c) The FTIR characterization, (d) Voltammogram of differential pulse characterization of SPCE bare 1) SPCE-CeO_2 2) SPCE CeO_2-Bioconjugate 3) SPCE-CeO_2-Bioconjugat-ENaC 4) using a redox system $K_3[Fe(CN)_6]$ 10 mM in KCl 0.1 M. Scan rate 0.008 V s^{-1} at potential range -1.0 V to +1.0 V

3.2. Modification of SPCE and its characteristics

Carbon-based electrodes such as SPCE are less selective, so modifications are needed to increase electrode selectivity for the target analyte. Therefore, the SPCE was modified with CeO_2 to obtain an excellent current response because it is a rare earth element with useful catalytic features and electrochemical properties. The good electrical conductivity of CeO_2 can

also increase electrode sensitivity and selectivity. CeO_2 attached to the electrode will undergo electrochemical reduction (electrodeposition) from Ce^{3+} to CeO_2 [12,34,37,38].

Bare SPCE, SPCE/CeO2, and SPCE/CeO_2/AuNP-aptamers were characterized by DPV by monitoring changes in the current response of 10 mM $[Fe(CN)_6]^{3-/4-}$ in 0.1 M KCl solution in the potential range –1.0 to +1.0 V and a scan rate of 0.008 V/s, as can be seen in Figure 2d**.** The AuNP-aptamer bioconjugate was immobilized onto the SPCE-CeO_2 electrode surface by passive adsorption, which is a simple immobilization method involving physically adsorbed species. CeO_2 is slightly negatively charged at neutral pH (ζ-potential = −6.2 mV). The aptamer can be adsorbed efficiently, an aptamer has a strong affinity with nanoceria [12,37,38]. The aptamer is negatively charged due to the presence of a phosphate group that can interact with positive amino acid residues (arginine, histidine, lysine). The interaction of aptamer with the ENaC protein is not only through electrostatic interactions but also by structural complementarity and hydrogen bonding. The aptamer-ENaC complex shows good complementarity [17]. The interaction between aptamer and ENaC was measured by DPV based on the transfer of electrons from $[Fe(CN)_6]^{3-/4-}$ as an electroactive species that undergo redox reactions. The bioconjugate is a large molecule and is not conductive. The addition of the bioconjugate to the SPCE/CeO_2 surface will inhibit the electron transfer resulting in a decrease in the peak $[Fe(CN)_6]^{3-/4-}$.

3.3. Experimental optimization according to the Box-Behnken method

Response surface methodology is an efficient statistical technique for the optimization of multiple variables to predict the best conditions employing a minimum number of experiments. The Box–Behnken experimental design was employed to obtain the optimum value of every factor. Three factors such as the concentration of aptamer ($\times_1$), incubation time of bioconjugate ($\times_2$), and protein incubation time of ENaC ($\times_3$) gave 15 times independent experiments with three different levels. The Box–Behnken design was set to two replication blocks for two repetitions; therefore, the number of total experiments is 30 times (data not shown). The results show that the factor with the most effect was the aptamer concentration (P-value < 0.05), with the coefficient of the response function calculated based on the following equation:

$$Y = 1.593 - 0.760 \times_1 + 0.0333 \times_2 - 0.089 \times_3 + 0.08 \times_{12} - 0.000932 \times_{22} + 0.00047 \times_{32} - 0.0006 \times_1\times_2 + 0.0884 \times_1\times_3 + 0.00004 \times_2\times_3 \quad (1)$$

where Y is the response in the current; $\times_1$, $\times_2$, and $\times_3$ represent the variable. The equation shows that the current response will be directly proportional to the bioconjugate incubation time, which is indicated by a constant value that is positive and shows that the bioconjugate incubation time has a synergistic effect on the ENaC aptasensor response.

Gothwal et al. stated that the incubation time is one of the kinetic factors that significantly impact the electrochemical biosensor signal process [39]. The Box-Behnken design results that the optimum conditions for each factor were an aptamer concentration of 0.5 μg mL^{-1}, a

bioconjugate incubation time of 30 minutes, and ENaC protein incubation time of 15 minutes. The P-value for the lack of fit was 0.297 or greater than 0.05, indicating that the resulting linear model is appropriate.

3.4. Aptasensor response to ENaC protein

The aptasensor response to ENaC was determined by DPV as shown in Figure 3a. Based on the characterization results, the higher the ENaC concentration, the lower the peak current produced because ENaC is a large and non-electroactive biomolecule, so the higher the concentration of ENaC, the more blocking of the electron transfer process of $[Fe(CN)_6]^{3-/4-}$. The calibration curve in Figure 3b shows that the linear regression equation Y= 0.168X + 0.614 with R^2 is equal to 0.996. The limit of detection (LOD) was evaluated using the blank signal, y_B, plus three times standard deviations of the blank, s_B. The y_B is the intercept of the calibration curve, and the s_B was obtained from the random errors in they-direction. The limit of quantification (LOQ) was evaluated using ten times the standard deviation of the blank [40]. The LOD and LOQ have appeared at the ENaC level of 0.110 and 0.365 ng mL^{-1}.

The comparison of LOD of the developed biosensors are in line with those previously reported in Table 2. The ENaC protein level in the normal urine sample for women is 2.1 ng mL^{-1} and men 1.35 ng mL^{-1} [4]. In this experiment, a LOD of 0.110 ng mL^{-1} was obtained, so that these results can still be used to differentiate ENaC levels in normal and hypertensive urine samples for both men and women, although LOD values are higher than previously reported studies [12,41].

Table 2. Several studies of electrochemical biosensors to detect ENaC protein

Biosensor	**Exposed area of Working Electrode (mm^2)**	**LOD**	**Reference**
Immunosensor based on AuNP-antiENaC bioconjugate on SPCE-Au	19.547	0.084 ng mL^{-1}	[7]
Immunosensor by using SPCE-rGO	19.547	0.198 ng mL^{-1}	[8]
Label free Immunosensor using SPCE-Au	19.547	0.037 ng mL^{-1}	[41]
Aptasensor by using SPCE-CeO_2 via electrodeposition	8.865	0.012 ng mL^{-1}	[12]
Aptasensor based on AuNP-aptamer bioconjugate on SPCE-CeO_2	8.865	0.110 ng mL^{-1}	This work

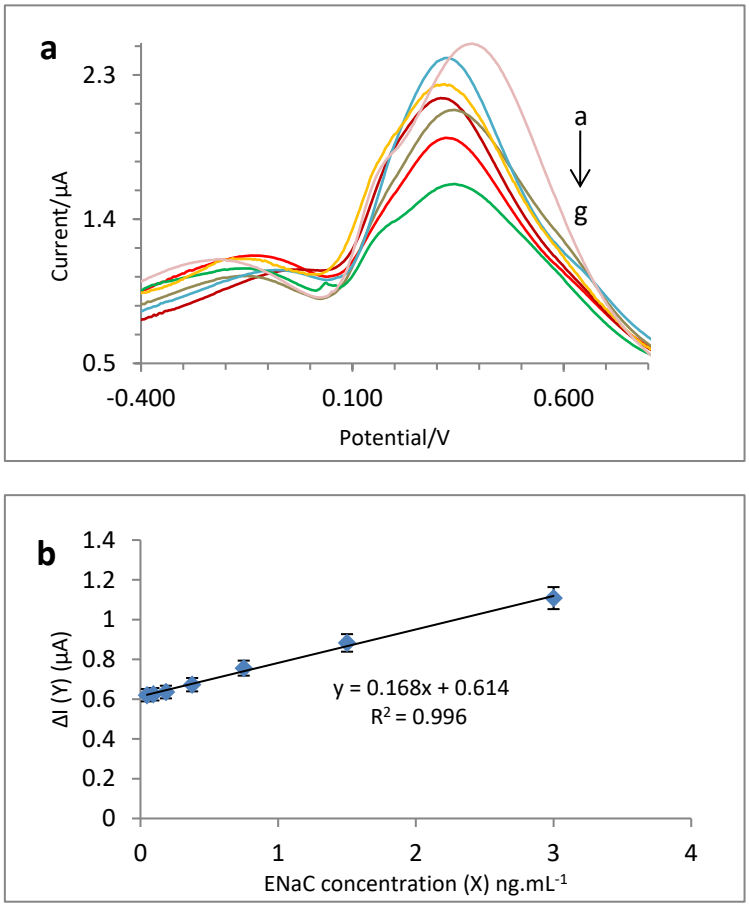

Figure 3. a) Differential pulse voltammogram for various ENaC concentrations a→g (0.047; 0.094; 0.187; 0.375; 0.75; 1.5; 3) ng.mL^{-1} measured with a redox system with $K_3[Fe(CN)_6]$ 10 mM solution in solution KCl 0.1. Scan rate 0.008 V/s over a potential range of -1.0 V up to +1.0 V, b) aptasensor ENaC calibration curve with various concentrations (0.047; 0.094; 0.187; 0.375; 0.75;1.5; 3) ng.mL^{-1} as measured by the redox system with $K_3[Fe(CN)_6]$ 10 mM solution in 0.1 KCl solution. Scan rate 0.008 V/s over a potential range of -1.0 V to +1.0 V

3.5. The Aptamer Selectivity

The graph of the decrease in the current response of $Fe(CN)_6$ for 3 repetitions of measurements is shown in Figure 4a. After the addition of ENaC protein to the aptamer, it showed a decrease in current of around 64.06%, this was due to the very good activity of the aptamer in recognizing ENaC protein as a target. Creatinine and potassium cchannels decreased current response by 24.84% and 8.17%, respectively. The decrease in current response is due to an interaction between Aptamer ENaC and each interference. However, in this case, the interaction that occurs is not significant because the resulting decrease in current is not greater than that of the ENaC protein and even has a high difference when compared to the decrease in the current response of the ENaC protein.

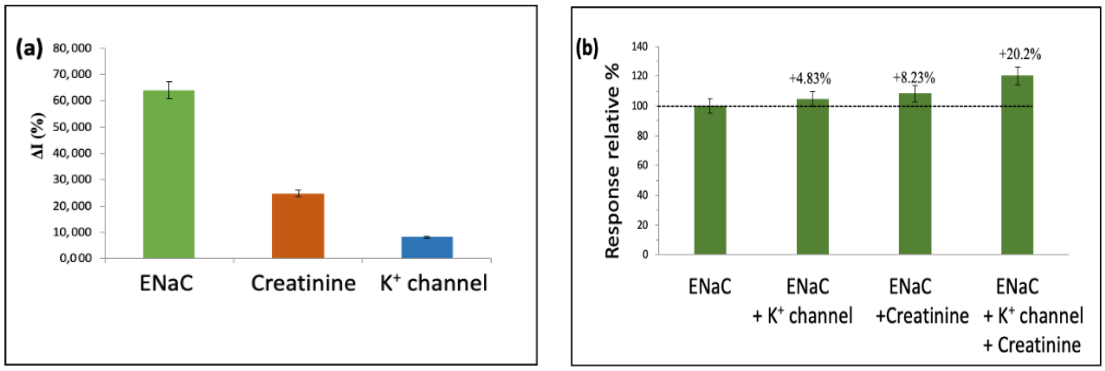

Figure 4. a) Graph of decreasing current of ENaC aptamer against ENaC protein, creatinine and K^+-channel, b) the changes in response when added protein creatinine and K^+-channel

Other treatments were reviewed to see the effect of interference in determining the percentage of selectivity. At the time of adding an interference (K^+ channel and creatinine) to the ENaC protein, Figure 4b shows the addition of the K^+ channel protein gave a change of less than 5% indicating no interference effect was produced [42]. Meanwhile, the addition of creatinine gave a change of 8.23% and when the three proteins were mixed it resulted in a change of 20.2%, in this case, the results of the ENaC Aptasensor selectivity study in vitro with the electrochemical method resulted in a selectivity percentage of 79.8% which indicates that there is interference or interference did not affect Aptamer measurement of ENaC protein.

3.6. The stability of Functionalized Ceria/AuNP-Streptavidin-Biotinylated Aptamer Screen-Printed Carbon Electrode

The stability of the biosensor was evaluated by comparing the slope of the calibration curve (related to sensitivity), looking at the change in the correlation coefficient (R^2) and determining the % RSD associated with the analyst's accuracy measured on different days. Stability studies were carried out by storing the ENaC aptasensor for 1 day, 15 days, 30 days and 60 days at room temperature, and 1 month at 50 °C which is equivalent to one year at room temperature [43].

Table 3 shows the stability of the ENaC aptasensor on the SPCE-CeO_2 surface, maintaining its initial sensitivity of 82.68% after one year from the first day of measurement with an R^2 value > 0.98, and a % RSD of 0.7. The % RSD obtained by 0.7 % represents a good sensor reproducibility because it is in accordance with the reproducibility suggested by the Association of Analytical Communities (AOAC) which is < 4%. The relationship between the protein concentration of ENaC ng/mL (X) and the current response A (Y) obtained an R^2 value of 0.988 within one year, this indicates that the magnitude of the ENaC concentration still affects the measured current response.

Table 3. ENaC Aptasensor stability results based on storage time at room temperature

Time	Slope	Linearity	RSD(%)
1 day	0.074	0,999	0.402
15 days	0.073	0,997	0.570
30 days	0.064	0,990	0.916
60 days	0,063	0,988	1.014
1 year	0.074	0,988	1.560

4. CONCLUSION

An aptasensor based on the AuNP-aptamer bioconjugate on SPCE-CeO_2 was developed for the rapid and direct quantification of ENaC in urine. The selectivity of the aptamer has been shown to be about 80% selective towards the ENaC protein with 20% interfering. Aptasensor storage shows stable results within a year, and possibly more than one year. This aptasensor has a low-level detection of ENaC that can still differentiate ENaC levels in normal and hypertensive urine samples for both men and women.

Acknowledgments

This research was funded by the Universitas Padjadjaran Academic Leadership Grant No. 1959/UN6.3.1/PT.00/2021, and the PDUPT Scheme Research of Indonesian Ministry of Research, Technology and the National Innovation Agency no. 1207/UN6.3.1/PT.00/2021.

REFERENCES

[1] V.P. Giena, S. Thongpat, and P. Nitirat, Int. J. Nurs. Sci. 5 (2018) 201.
[2] B.M. Egan, J. Am. Heart Assoc. 7 (2018) e009971.
[3] [Online] available at: World Health Organization (WHO), A global brief on hypertension (2013) Available Source:apps.who. int/iris/bitstream/ 10665/79059/1/ WHO_ DCO_ 2013.2
[4] Y. Sofiatin, and M.A. Roesli, Am. J. Clin. Med. Res. 6 (2018) 20.
[5] I. Hanukoglu, and A. Hanukoglu, Gene. 579 (2016) 95.
[6] D.J. Benos, and B.A. Stanton, J. Phys. 520 (1999) 631.
[7] Y.W. Hartati, S. Gaffar, D. Alfiani, U. Pratomo, Y. Sofiatin, T. Subroto, and T. Sens. Biosens. Res. 29 (2020) 100343.
[8] Y.W. Hartati, S.F. Yusup, Fitrilawati, S. Wyantuti, Y. Sofiatin, and S. Gaffar, Curr.Chem. Lett. 9 (2020) 151.
[9] A.L Pitzer, J.P. Van Beusecum, T.R. Kleyman, and A. Kirabo, Curr Hypertens. Rep. 22 (2020) 1.
[10] E. Jones, and B. Rayner, Pediatr Nephrol. 36 (2021) 237.

[11] D.L. García-Rubio, M.B. de la Mora, D.Cerecedo, J.m.S. Blesa, and M. Villagrán-Muniz, Biosens. Bioelectron. 157 (2020) 112151.
[12] Y.W. Hartati, D.R. Komala, D. Hendrati, S. Gaffar, A. Hardianto, Y.Sofiatin, and H.H. Bahti, Soc. Open Sci. 8 (2021) 202040.
[13] M.H. Ali, M.E. Elsherbiny, and M. Emara, Int. J. Mol. Sci. 20 (2019) 2511.
[14] Y. Wang, G. Zhao, G. Zhang, Y. Zhang, H. Wang, W. Cao, T. Li, and Q. Wei, Sens. Actuators B 319 (2020) 128313.
[15] W. Kong, F. Qu, and L. Lu, Anal. Bioanal. Chem. 412 (2020) 841.
[16] A. Verdian, Z. Rouhbakhsh, and E. Fooladi, J. Hazzard. Mater. 402 (2021) 123531.
[17] D.R. Komala, A. Hardianto, S. Gaffar, and Y.W. Hartati, Pharm. Sci. 27 (2021) 67.
[18] V.B. Borse, A.N. Konwar, R.D. Jayant, and P.O. Patil, Drug Deliv. Transl. Res. 10 (2020) 878.
[19] M. Emami, M. Shamsipur, R. Saber, and R. Irajirad, Analyst. 139 (2014) 858.
[20] Y.W. Hartati, D. Nurdjanah, S. Wyantuti, A. Anggraeni, and S. Gaffar, AIP Conf. Proc. 2049 (2018) 020051.
[21] Y.W. Hartati, L. Letelay, S. Gaffar, S. Wyantuti, and H.H. Bahti, Sens. Biosens. Res. 27 (2020) 100316.
[22] A.Rhouati, J.L. Marty, and A. Vasilescu, Nanotech. Biosens. 1 (2018) 193.
[23] Y. Roupioz, J. Chem. Edu. 96 (2019) 1002.
[24] L. Garc, Introducing gold nanoparticle bioconjugates within the biological machinery. Thèse (2013) pp. 235.
[25] E.I. Fazrin, A.I. Naviardianti, S. Wyantuti, S. Gaffar, and Y.W. Hartati, PENDIPA J. Sci. Edu. 4 (2020) 1.
[26] R. D'Agata, P. Palladino, G. Spoto, G. Beilsten. J. Nanotechnol. 8 (2017) 1.
[27] T. Fellows, L. Ho, S. Flanagan, R. Fogel, D. Ojo, and J. Limson, Analyst 145 (2020) 5180.
[28] Y. You, S. Lim, and S. Gunasekaran, ACs Appl. Nano Mater. 3 (2020) 1900.
[29] D.Wu, H. Lu, Jirul Wang, L. Wu, L. Liu, X. Yi, X., Jianxiu Wang, and H. Tang, Microchem. J. 164 (2021) 106066.
[30] J. Calvache-Muñoz, F.A. Prado, and J.E Rodríguez-Páez, Colloids Surf. A 529 (2017) 146.
[31] J. Fu, Q. Zhang, Z. Shi, Y. Guo, F. Li, Y. Zhang, and X. Sun, Int. J. Electrochem. Sci. 13 (2018) 9231.
[32] N. Pongpichayakul, S. Themsirimongkon, S. Maturost, K. Wangkawong, L. Fang, B. Inceesungvorn, P. Waenkaew, and S. Saipanya, Int. J. Hydrog. Energy. 46 (2021) 2905.
[33] F. Charbgoo, M. Ramezani, and M. Darroudi, Biosens Bioelectron. 96 (2017) 33.
[34] Y.W. Hartati, S.N. Topkaya, S. Gaffar, H.H. Bahti, and A.E. Cetin, RSC Adv. 11 (2021) 16216.

[35] P. Zhao, N. Li, and D. Astruc, Coord. Chem. Rev. 257 (2013) 638.
[36] M. Jarczewska, A. Trojan, M. Gągała, and E. Malinowska, Electroanalysis 31 (2019) 1125.
[37] M. Y.M. Abdelrahim, S.R. Benjamin, L.M. Cubillana-Aguilera,I. Naranjo-Rodríguez, J.L. Hidalgo-Hidalgo de cisneros, J.J. Delgado, and J.M. Palacios-Santander, Sensors 13 (2013) 4979.
[38] B. Liu, Z. Sun, P.J.J. Huang, and J. Liu, J.Am. Chem. Soc. 137 (2015) 1290.
[39] A. Gothwal, P. Beniwal, V. Dhull, and V. Hooda, J. Anal. Chem. 2014 (2014) 303641.
[40] J.N. Miller, J. Miller, Statistics and Chemometrics for Analytical Chemistry (2010) 6th Edition.
[41] Y.W.Hartati, N. P. Satriana, S. Gaffar, J.Y. Mulyana, S. Wyantuti, and Y. Sofiatin, Eur. J (2020).
[42] M.H Mat Zaid, J. Abdullah, N, Rozi, A.A. Mohamad Rozlan, and S. Abu Hanifah, Nanomaterials. 10 (2020) 1346.
[43] [Online] available at: https://www.biologydiscussion.com/immunology/reagent-formulation/reagent formulation-and-shelf-life-evaluation-products-immunology/ 84841. Accesed 13-12-2021.